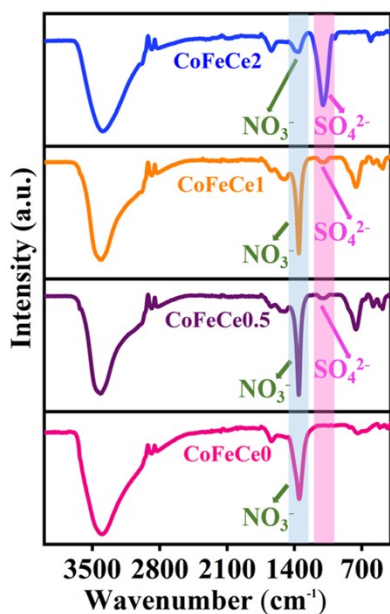


Pore Size and Electronic Tuning in Cerium-doped CoFe-LDH for Oxygen Evolution Reaction

Parul Aggarwal, Bhupendra Singh, and Amit Paul*

Department of Chemistry, Indian Institute of Science Education and Research Bhopal, Bhopal Bypass Road, Bhopal, M.P-462066 (India) (Email: apaul@iiserb.ac.in)

Figure/ Table No.	Contents	Page No.
Figure S1 Table S1	FTIR spectra, functional group analysis	S2
Figure S2	TGA plots for all LDHs	S2
Figure S3	EDS Spectra and elemental mapping for all LDHs	S3
Figure S4	SAED pattern of Ce-doped CoFe LDHs.	S4
Figure S5	HRTEM images of Ce-doped CoFe LDHs showing lattice fringes	S4
Figure S6	XPS Spectrum of Ce-doped CoFe LDHs	S5
Figure S7	Cumulative pore volume for all LDHs	S5
Figure S8	Electrochemical results of CoFeCe ₂ and CoFeCe ₃ LDHs	S6
Figure S9	CVs in non-faradaic potential region for all LDHs	S6
	Areal capacitance, ECSA and RF determination methodology	S7
Figure S10	Equivalent circuit model for AC Impedance	S8
Figure S11	24-hour Chronoamperometry and O ₂ quantification	S8
Figure S12	Post-catalysis SEM	S9
Figure S13	EDS spectrum before and after electrocatalysis	S9
Figure S14	Elemental mapping before and after electrocatalysis	S10
Figure S15	PXRD and XPS after electrocatalysis	S11
Table S2	Ratio of Co ³⁺ /Co ²⁺ in different LDHs.	S11
Table S3	Cumulative pore volume in different pore size ranges of LDHs	S11
Table S4	Average diameter of large nucleates in different LDHs	S12
Table S5	Literature comparison of recently studied LDH-based material for OER	S12
Table S6	Non-faradic capacitances (C _{dl}), electrochemically accessible surface areas (ECSA), and surface roughness factors (RF) of Ce-doped CoFe LDHs.	S13
Table S7	Equivalent circuit fitted parameters	S13
	Reference	S13



Functional Group	Wavenumber (cm ⁻¹)
Stretching vibration of hydroxyl groups in the interlayer	~3400
Bending vibration of water molecules (hydrogen-oxygen-hydrogen bending vibration) which implied the presence of adsorbed water in the structures	~1600
NO ₃ ⁻	1362
SO ₄ ²⁻	1107
Stretching vibrations of M-O	~755
Stretching vibrations of M-O-M	~470

Figure & Table S1: FTIR spectra and functional group analysis of Ce-doped CoFe LDHs.

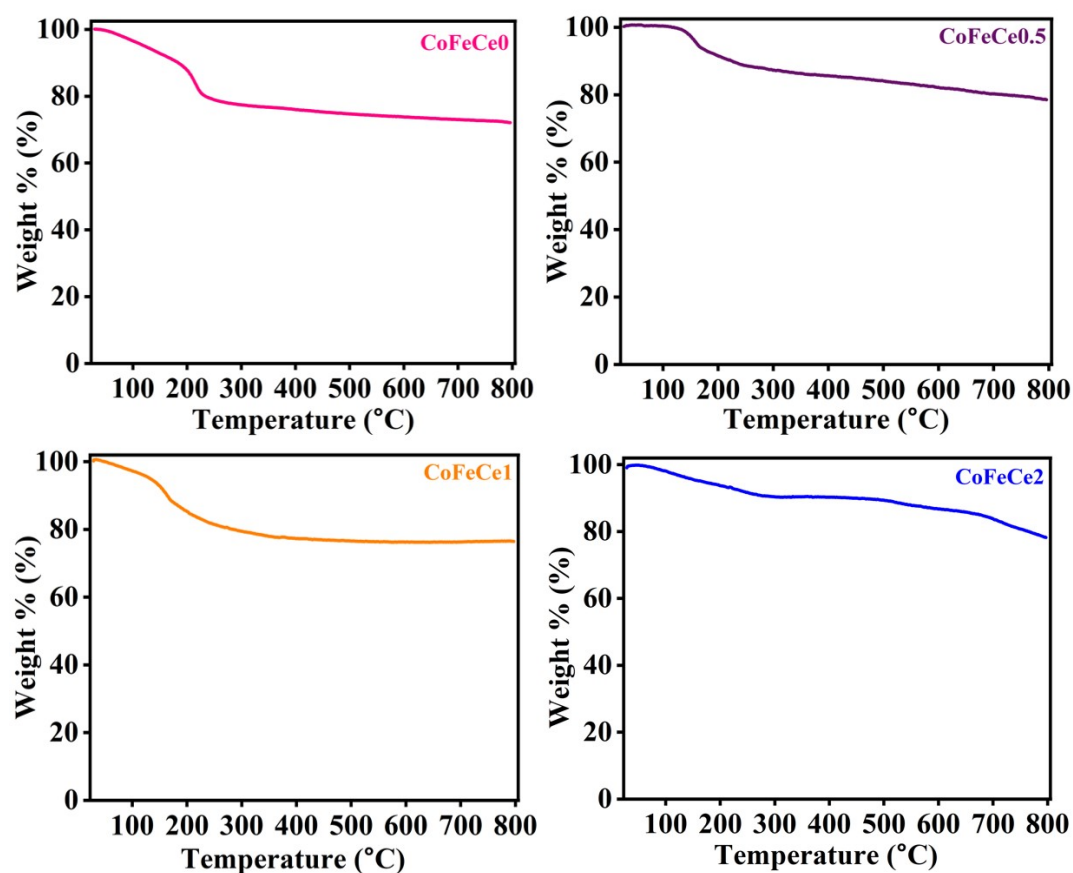


Figure S2: TGA plots of Ce-doped CoFe LDHs.

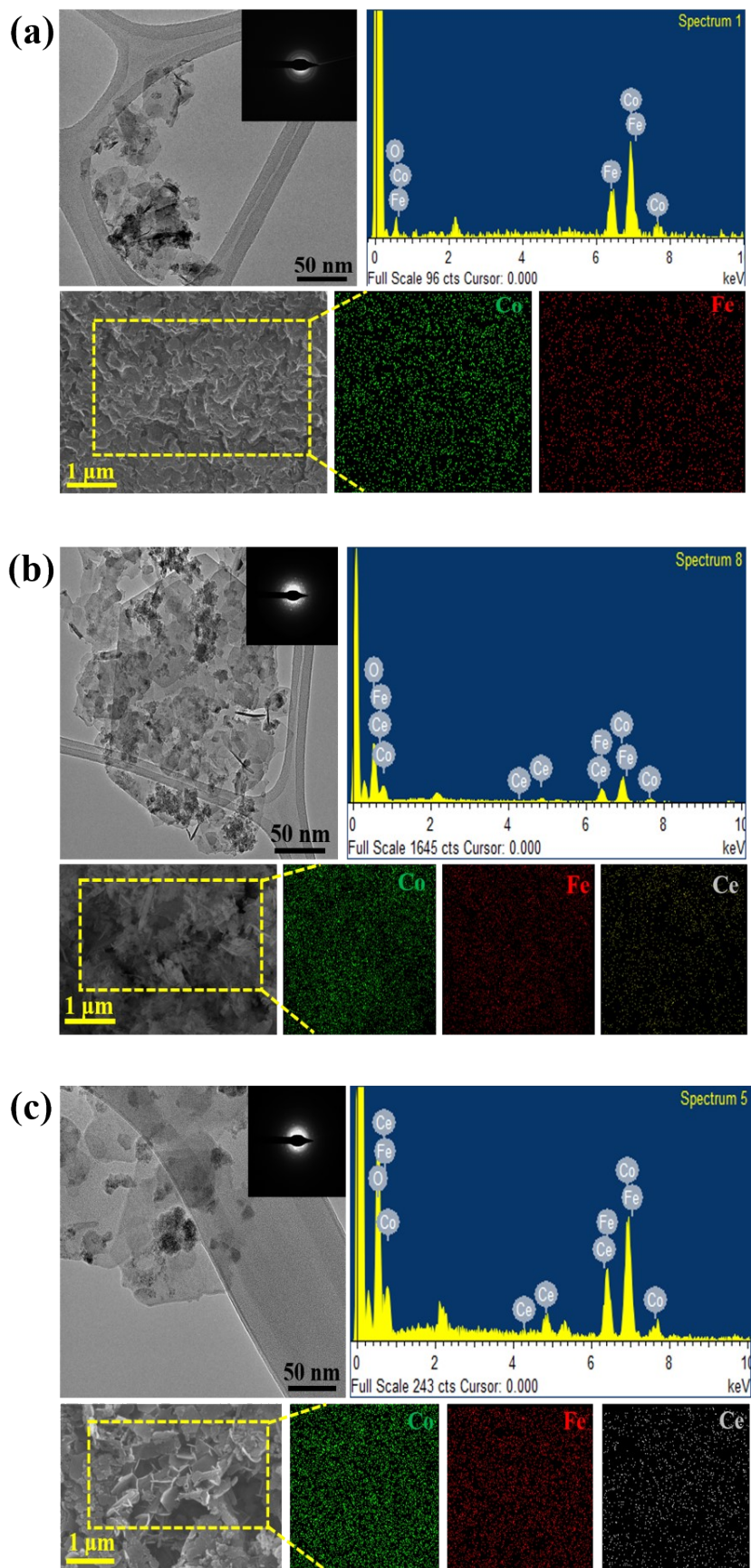


Figure S3: A low-resolution TEM micrograph of (a) CoFeCe₀, (b) CoFeCe_{0.5} and (c) CoFeCe₁ LDHs along with EDX spectra and elemental mappings.

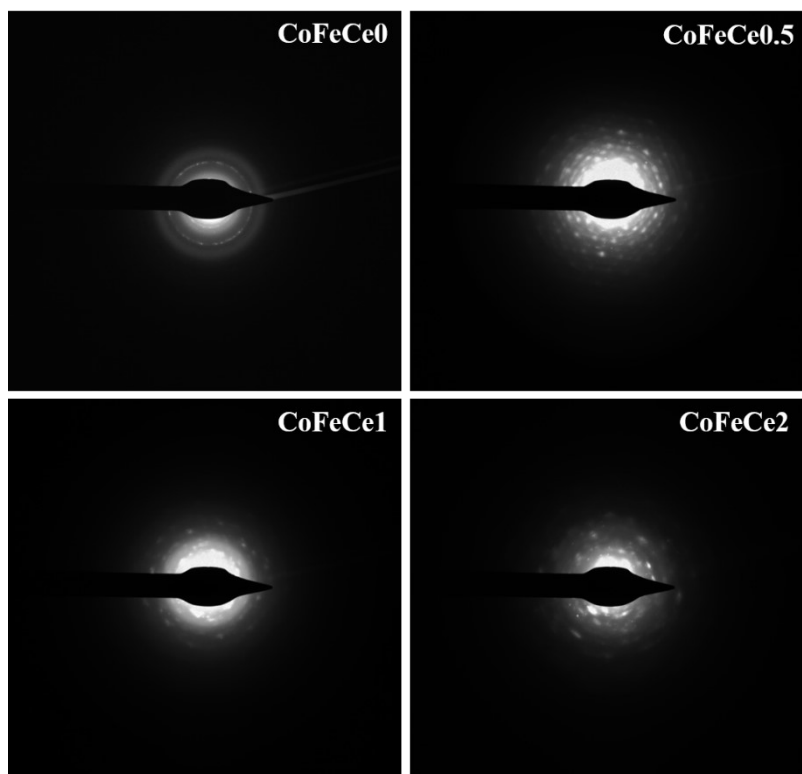


Figure S4: SAED pattern of Ce-doped CoFe LDHs.

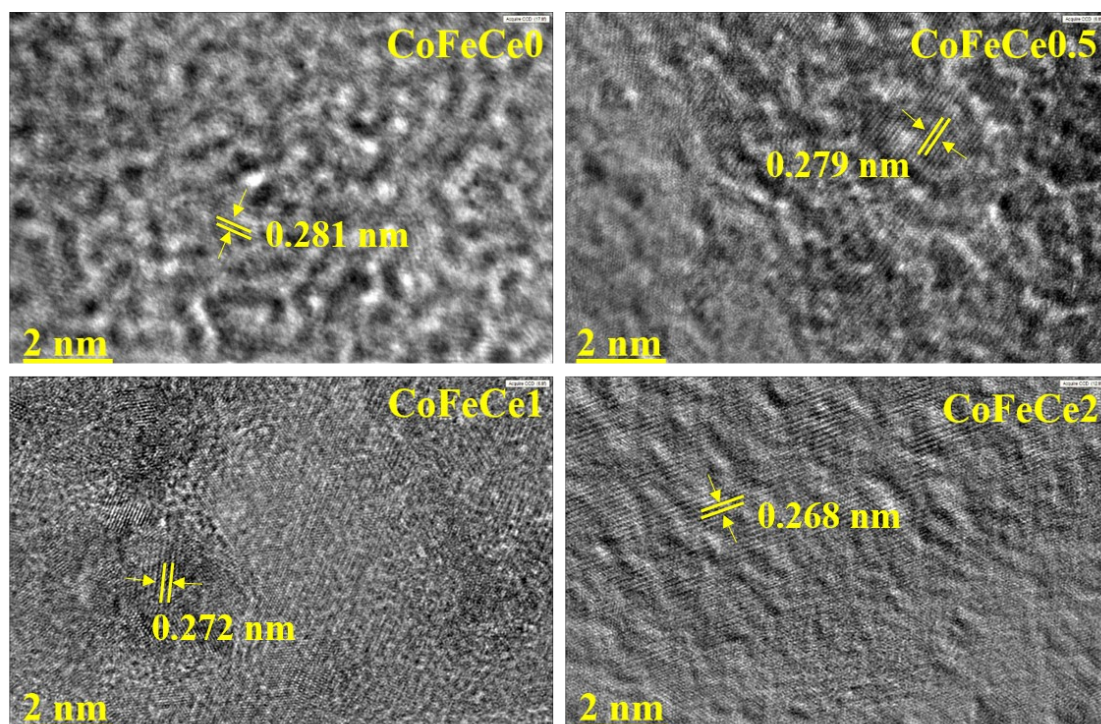


Figure S5: HRTEM images of Ce-doped CoFe LDHs showing lattice fringes.

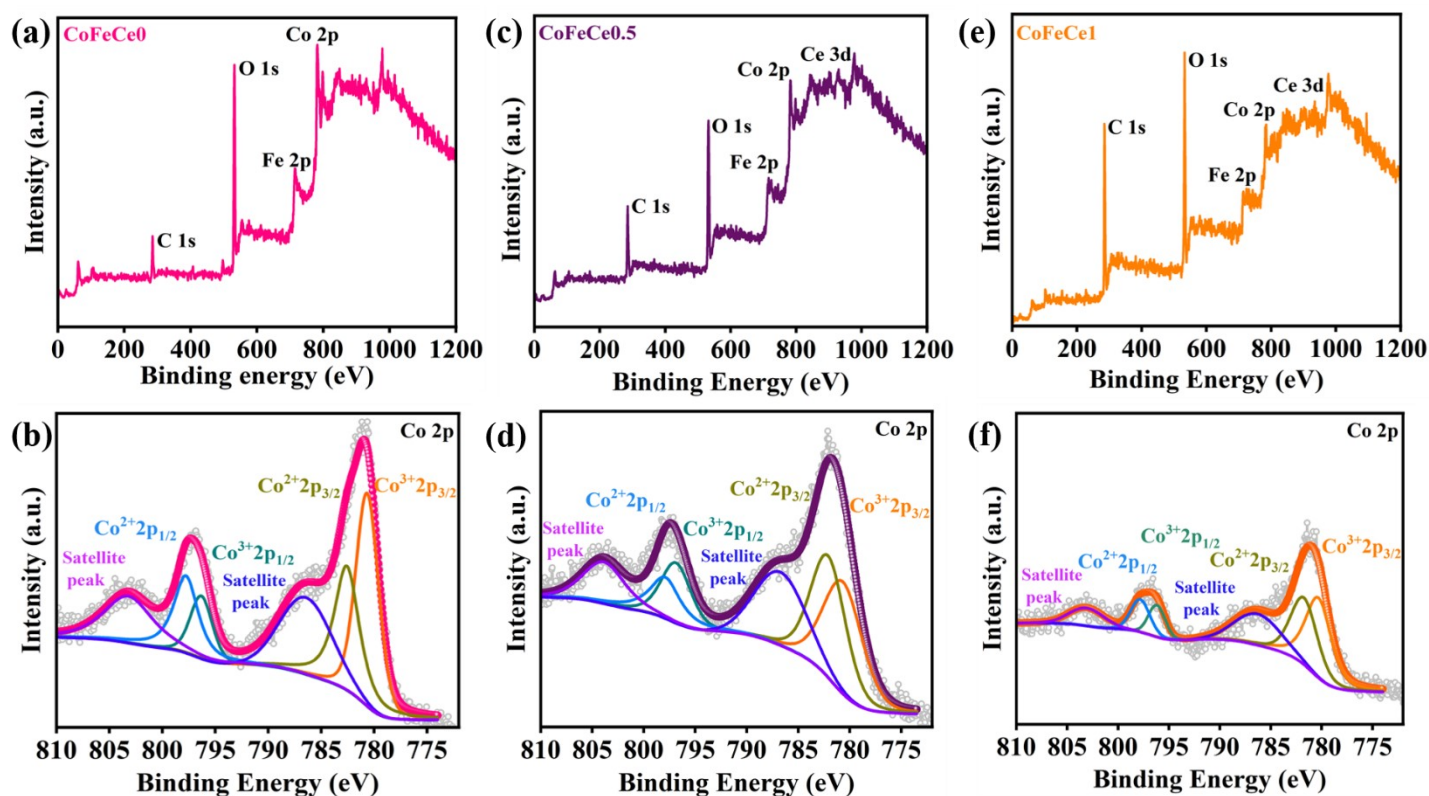


Figure S6: (a-c) XPS spectrum, and (d-f) deconvoluted Co 2p spectrum for **CoFeCe0**, **CoFeCe0.5** and **CoFeCe1** LDH respectively.

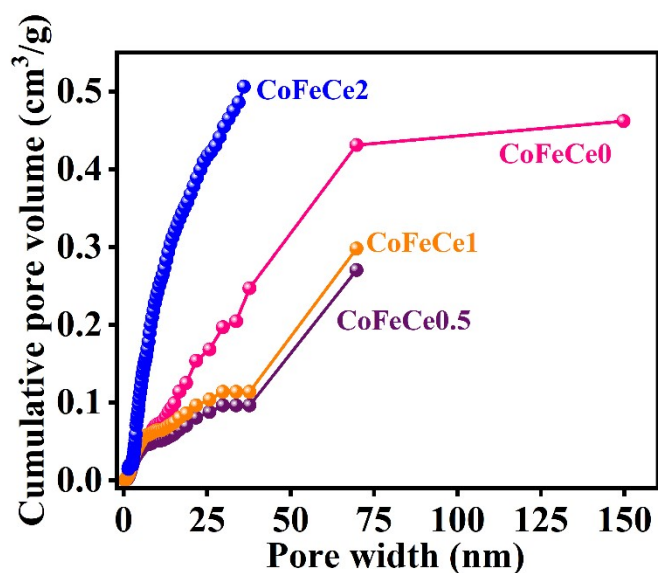


Figure S7: Cumulative pore volume for **CoFeCe0**, **CoFeCe0.5**, **CoFeCe1** and **CoFeCe2** LDH respectively.

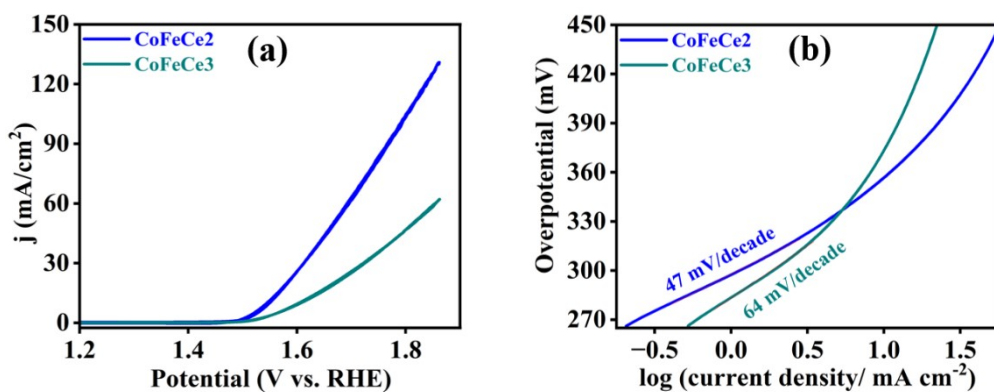


Figure S8: Electrochemical results of LDHs. (a) CVs at scan rate of 5 mV s⁻¹ and (b) Tafel plots of CoFeCe2 and CoFeCe3 LDHs during water oxidation.

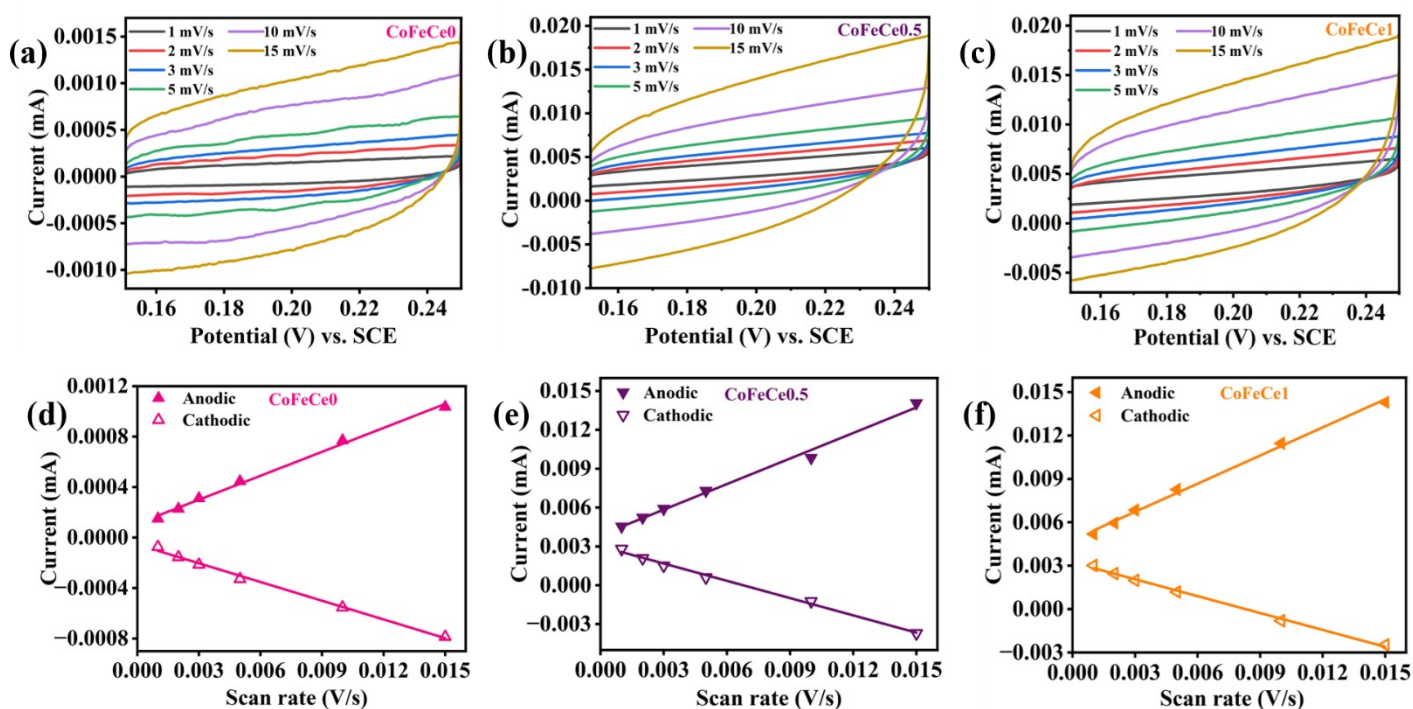


Figure S9: (a-c) CVs at different scan rate in a non-faradaic potential region (0.15 to 0.25 V versus SCE) for Ce-doped CoFe LDHs and (d-f) Plot of anodic and cathodic charging currents at 0.2 V (vs. SCE) vs. scan rate of voltammetry

Calculation of areal capacitance (C_{dl} , $\mu\text{F}/\text{cm}^2$), electrochemically accessible surface area (ECSA) and roughness factor (RF)

The charging current for cathodic (i_c) and anodic (i_a) currents were taken at 0 V *versus* Ag/AgCl. The relation between i_c/i_a *versus* scan rate (ν) and the double layer capacitance (C) was given by equations S1 (a-b).

$$i_a = \nu * C \dots\dots\dots(S1a)$$

$$i_c = \nu * C \dots\dots\dots(S1b)$$

The slopes of i_c and i_a as a function of ν provided C from the slope. The average slope calculated from cathodic and anodic currents was taken as C . The geometrical area of the electrode (GSA) was 0.07 cm^2 . The areal capacitances (C_{dl} , $\mu\text{F}/\text{cm}^2$) were calculated by dividing C with GSA. For the calculation of electrochemically accessible surface area (ECSA), equation S2 has been used wherein $C_s=40 \mu\text{F}/\text{cm}^2$ (specific surface area) is taken from the literature.¹

$$\text{ECSA} = C/C_s \dots\dots\dots (S2)$$

Roughness factor (RF) was estimated using equation S3.

$$\text{Roughness Factor (RF)} = \text{ECSA}/\text{GSA} \dots\dots\dots (S3)$$

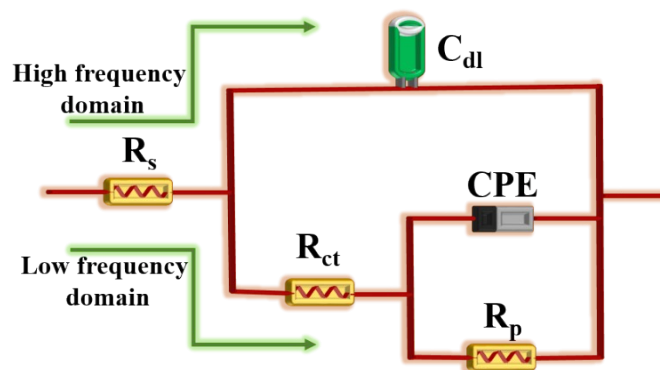


Figure S10: Equivalent circuit model used for fitting OER catalysis results by Ce-doped CoFe LDHs. R_s , C_{dl} , R_{ct} , R_p , and CPE represent uncompensated solution resistance, double-layer charging at the electrode/electrolyte interface at the high-frequency domain, charge transfer resistance at the electrode/electrolyte interface related to the overall OER, pseudoresistance, which is related to one or more surface intermediates formation, and pseudocapacitance which represents the change in charged surface species as OER proceeds respectively.

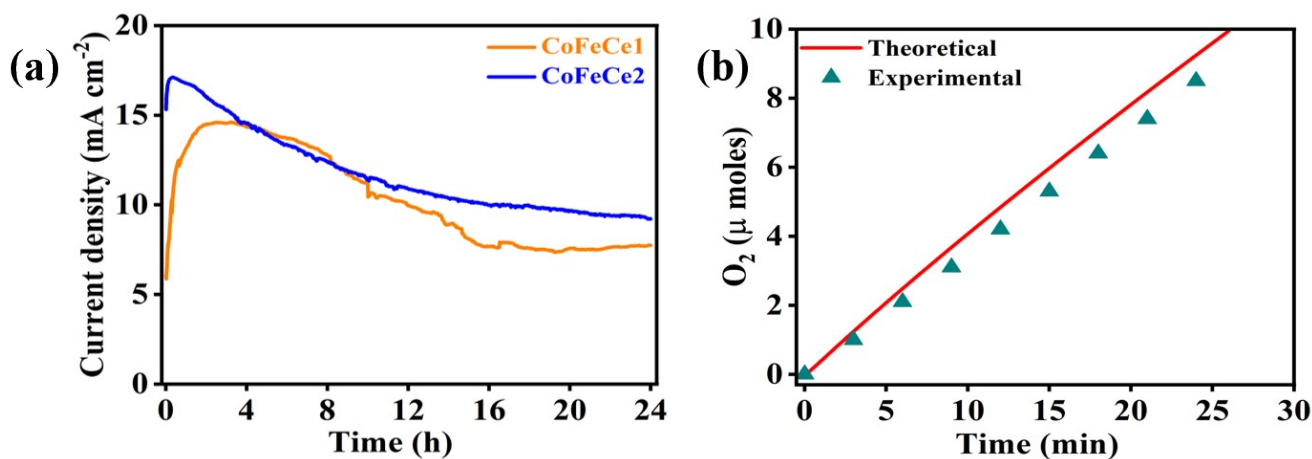


Figure S11: (a) Chronoamperogram showing the stability up to 24 h of CoFeCe1 and CoFeCe2 LDH at a constant potential of 1.63 V (vs. RHE) and (b) theoretical (cyan line) and experimental (cyan triangle) quantification of O₂ evolution of CoFeCe2 LDH at a constant potential of 1.54 V (vs. RHE) in 1 M KOH during water oxidation.

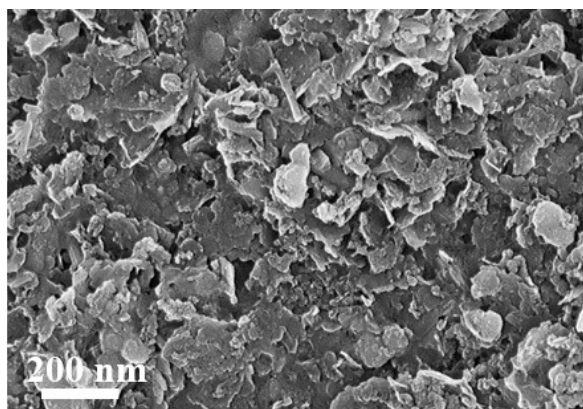


Figure S12: SEM image of **CoFeCe₂** LDH after 24 h chronoamperometry experiment at 1.54 V (vs. RHE) in 1 M KOH solution.

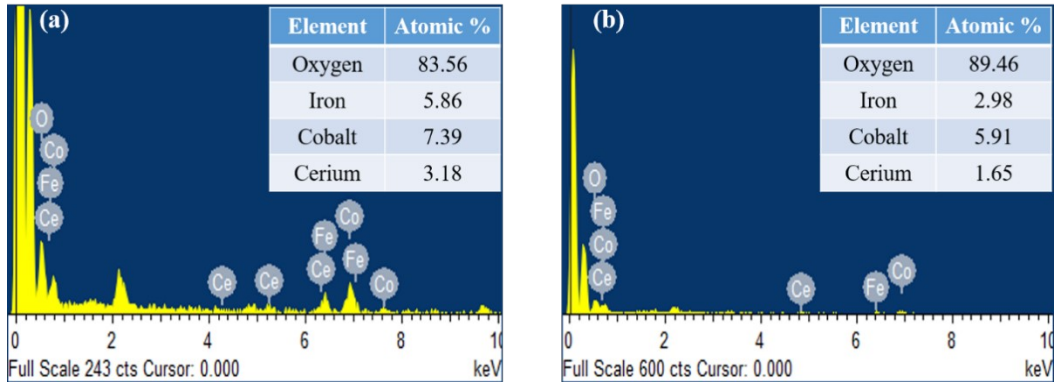


Figure S13: (a) and (b) Precatalysis and postcatalysis EDS spectrum of **CoFeCe₂** LDH coated on ITO glass substrate after 24 h chronoamperometry at 1.54 V (versus RHE) in 1 M KOH solution.

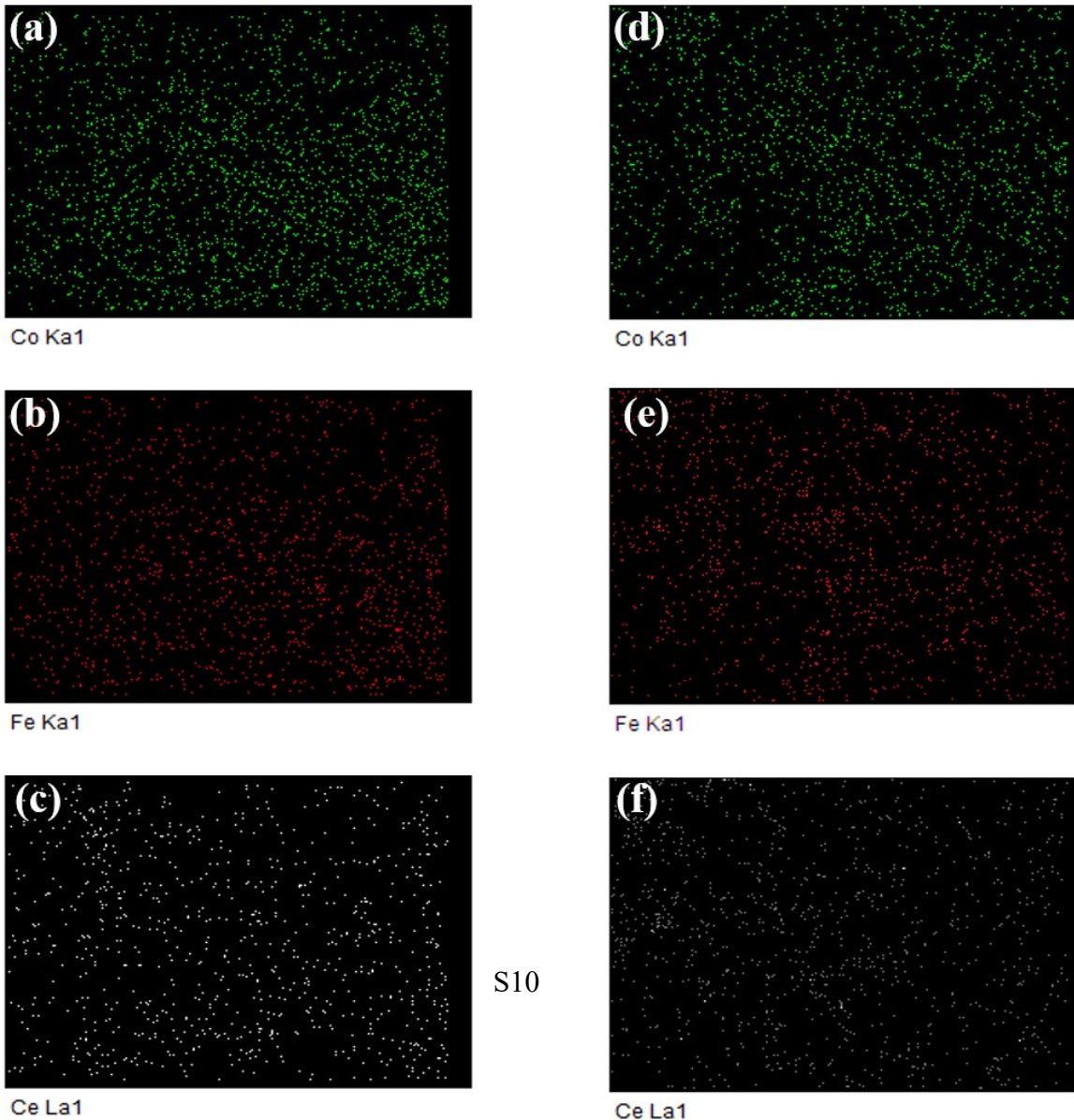


Figure S14: (a-c) and (d-f) Precatalysis and postcatalysis elemental mapping of **CoFeCe₂ LDH** after 24 h chronoamperometry at 1.54 V (versus RHE) in 1 M KOH solution.

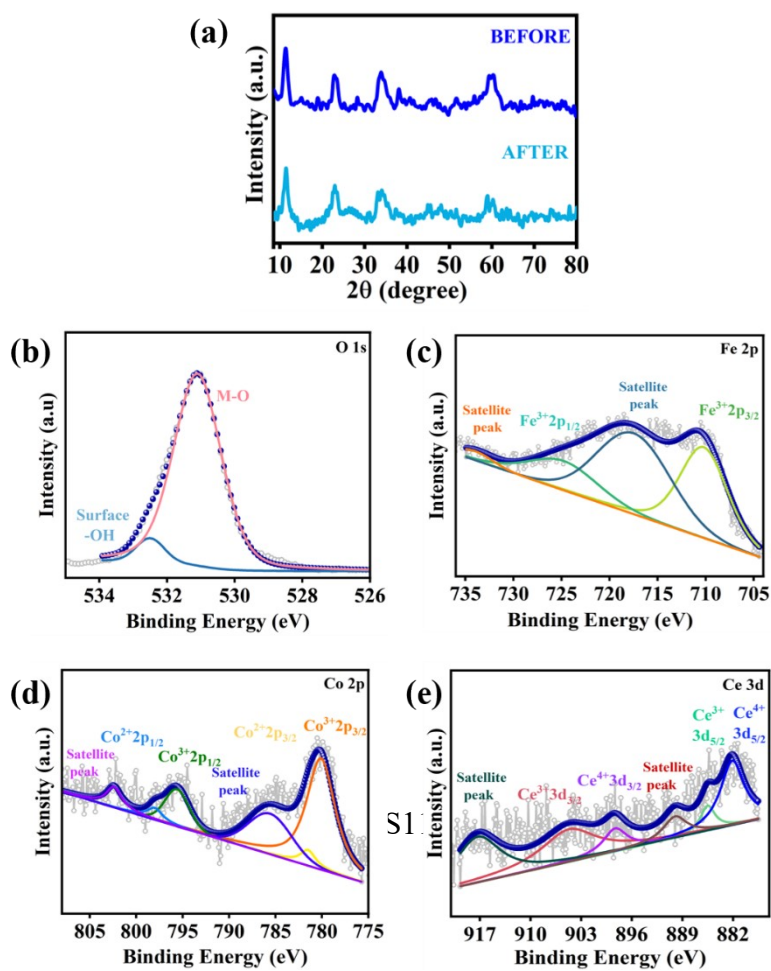


Figure S15: (a) Precatalysis and postcatalysis XRD and (b-e) XPS of **CoFeCe2** LDH after 24 h chronoamperometry at 1.54 V (versus RHE) in 1 M KOH solution.

Table S2: Ratio of $\text{Co}^{3+}/\text{Co}^{2+}$ in different LDHs.

SAMPLE	CoFeCe0	CoFeCe0.5	CoFeCe1	CoFeCe2
$\text{Co}^{3+}/\text{Co}^{2+}$	1.01	1.06	1.14	1.42

Table S3: Cumulative pore volume in different pore size ranges of LDHs.

SAMPLE	Pore volume ($\text{cm}^3 \text{g}^{-1}$) (0-2 nm)	Pore volume ($\text{cm}^3 \text{g}^{-1}$) (2-5 nm)	Pore volume ($\text{cm}^3 \text{g}^{-1}$) (> 5 nm)
CoFeCe0	0.012	0.033	0.395
CoFeCe0.5	0.011	0.028	0.321
CoFeCe1	0.015	0.035	0.330
CoFeCe2	0.019	0.102	0.390

Table S4: Average diameter of large nucleates in different LDHs.

SAMPLE	CoFeCe0	CoFeCe0.5	CoFeCe1	CoFeCe2
Average diameter (nm)	8.85 ± 1.36	10.73 ± 1.29	11.12 ± 1.55	13.31 ± 1.93

Table S5: Literature comparison of recently studied LDH-based material for OER.²⁻¹⁰

Catalysts	TOF (s ⁻¹)	Mass activity (A g ⁻¹)@ η =350 mV	Electrolyte	Reference
Ni _{0.66} Fe _{0.33} LDH	1.38 * 10 ⁻¹ @ 400 mV	-	1 M KOH	<i>Mater. Chem. Phys.</i> , 2020, 254 , 123496
Co ₃ Fe ₁ LDH	3.12 * 10 ⁻¹ @ 420 mV	-	1 M KOH	<i>ACS Appl. Mater. Interfaces</i> , 2019, 11 , 30887-30893
NiFe LDH	2.5 * 10 ⁻¹	141.2	1 M KOH	<i>Chem. Commun.</i> , 2020, 56 , 8770
Co ₂ Fe ₁ LDH	1.6 * 10 ⁻² @ 300 mV	-	1 M KOH	<i>ChemPlusChem</i> , 2017, 82 , 3, 483-488
CoFe ₂ O ₄ NSs	9.5 * 10 ⁻² @ 350 mV	-	1 M KOH	<i>J. Mater. Chem. A</i> , 2019, 7 , 7328-7332
O-NiCoFe-LDH	1.7 * 10 ⁻² @ 300 mV	-	0.1 M KOH	<i>Adv. Energy Mater.</i> , 2015, 5 , 1500245
Fe _{0.33} Co _{0.67} OOH PNSAs/CFC	1.42 * 10 ⁻² @ 300 mV	-	1 M KOH	<i>Angew. Chem. Int. Ed.</i> , 2018, 57 , 2672-2676
CoFe ₂ O ₄ nanospheres	2.12 * 10 ⁻³ @ 275 mV	-	1 M KOH	<i>CrystEngComm</i> , 2020, 22 , 4317-4323
(FeCoNiCrMn) ₃ O ₄ - 400	1.59 * 10 ⁻¹ @ 400 mV	67.3 @ 400 mV	1 M KOH	<i>Sustainable Energy Fuels</i> , 2022, 6 , 1479-1488
CoFeCe2 LDH	1.823	294.15	1 M KOH	This Work

Table S6: Non-faradic capacitances (C_{dl}), electrochemically accessible surface areas (ECSA), and surface roughness factors (RF) of Ce- doped CoFe LDHs.

SAMPLE	Capacitance C_{dl} (mF cm ⁻²)	ECSA (cm ²)	Roughness Factor (RF)
CoFeCe0	0.8	1.41	19.9

CoFeCe0.5	7.3	12.96	183.3
CoFeCe1	7.8	13.78	194.9
CoFeCe2	17.3	30.57	432.4

Table S7: Equivalent circuit parameters calculated from EIS fitting for all nanomaterials at 1.58 V (vs. RHE) in the frequency range from 10^5 to 10^{-1} s⁻¹ with 0.005 V amplitude.

SAMPLE	R_S (Ω)	R_{ct} (Ω)	C_{dl} (μF)	R_P (Ω)	Q (Fs^(a-1))	Exp (a)
CoFeCe0	10.1	8.1	0.027	74.6	0.00013	0.62
CoFeCe0.5	9.2	7.3	0.033	96.3	0.00006	0.76
CoFeCe1	11.2	7.4	0.038	52.1	0.00032	0.54
CoFeCe2	16.1	3.9	0.257	45.5	0.00025	0.63

References:

1. C. C. L. McCrory, S. Jung, J. C. Peters and T. F. Jaramillo, *J. Am. Chem. Soc.*, 2013, **135**, 16977-16987.
2. J. Long, J. Zhang, X. Xu and F. Wang, *Mater. Chem. Phys.*, 2020, **254**, 123496.
3. C. Ye, M.-Q. Wang, S.-J. Bao and C. Ye, *ACS Appl. Mater. Interfaces*, 2019, **11**, 30887-30893.
4. J. Saha, A. Kumar, A. Pm and V. Jakhad, *Chem. Commun.*, 2020, **56**, 8770-8773.
5. L. Feng, A. Li, Y. Li, J. Liu, L. Wang, L. Huang, Y. Wang and X. Ge, *ChemPlusChem*, 2017, **82**, 483-488.
6. H. Fang, T. Huang, D. Liang, M. Qiu, Y. Sun, S. Yao, J. Yu, M. M. Dinesh, Z. Guo, Y. Xia and S. Mao, *J. Mater. Chem. A*, 2019, **7**, 7328-7332.
7. L. Qian, Z. Lu, T. Xu, X. Wu, Y. Tian, Y. Li, Z. Huo, X. Sun and X. Duan, *Adv. Energy Mater.*, 2015, **5**, 1500245.
8. S.-H. Ye, Z.-X. Shi, J.-X. Feng, Y.-X. Tong and G.-R. Li, *Angew. Chem. Int. Ed.*, 2018, **57**, 2672-2676.
9. D. Guo, H. Kang, P. Wei, Y. Yang, Z. Hao, Q. Zhang and L. Liu, *CrystEngComm*, 2020, **22**, 4317-4323.
10. C. Duan, X. Li, D. Wang, Z. Wang, H. Sun, R. Zheng and Y. Liu, *Sustainable Energy Fuels*, 2022, **6**, 1479-1488.